Journal of Cellular Physiology

Effect of rMnSOD on Survival Signaling in Pediatric High Risk T-Cell Acute Lymphoblastic Leukaemia

A. PICA,[1]* A. DI SANTI,[1] V. D'ANGELO,[2] A. IANNOTTA,[2] M. RAMAGLIA,[2] M. DI MARTINO,[2] M.L. POLLIO,[1] A. SCHIATTARELLA,[3] A. BORRELLI,[3] A. MANCINI,[4] P. INDOLFI,[2] AND F. CASALE[2]

[1]*Department of Biology, University of Naples Federico II, Naples, Italy*

[2]*Department of Woman, Child and General and Specialized Surgery, Pediatric Oncology Service—Second University of Naples, Naples, Italy*

[3]*Molecular Biology and Viral Oncology Unit, Department of Experimental Oncology, "Istituto Nazionale Tumori Fondazione G. Pascale"—Irccs, Naples, Italy*

[4]*LaedhexaBiotechnologies Inc. QB3 Partners, San Francisco, California*

Manganese superoxide dismutase (MnSOD) is a mitochondrial enzyme that defends against oxidative damage due to reactive oxygen species (ROS). A new isoform of MnSOD with cytotoxic activity was recently discovered in liposarcoma cells. Here, we tested the effectiveness of a recombinant form of this isoform (rMnSOD) on leukemic T cells, Jurkat cells, and lymphocytes. Our results confirm that leukemic T cells can internalize rMnSOD and that rMnSOD causes apoptosis of 99% of leukemic cells without showing toxic effects on healthy cells. Using light and electron microscopy, we determined that an rMnSOD concentration of 0.067 μM most effective on apoptosis induction. Western blot analysis showed that treatment with 0.067 μM rMnSOD resulted in high expression of the pro-apoptotic protein Bax and low expression of the anti-apoptotic protein Bcl-2 in leukemia cells. Concerning signal transduction pathway no influence was observed after treatment except for Jurkat cells showing a slightly decreased expression of ERK phosphorylation. These results suggest that rMnSOD may be an effective and non-toxic treatment option for T-cell leukemia.

J. Cell. Physiol. 230: 1086–1093, 2015.

Leukemia is the most common childhood malignancy worldwide. Extensive evidence has shown that disturbances of oxidative stress metabolism are a common feature of transformed tumor cells (Skarstein et al., 2000). Both alterations of antioxidants and increases in the production of oxygen reactive species play a role in several stages of carcinogenesis (Malyszczak et al., 2005). Radical-mediated DNA damage resulting from the "oxidative damage" incidents leads to arrest or induction of transcription signal transduction pathways, replication errors and genomic instability and represents the first step involved in mutagenesis, carcinogenesis and ageing (Cooke et al., 2003 Valko et al., 2006).

Leukemic cells produce higher amounts of ROS than non-leukemic cells, as they are under a repeated state of oxidative blockade (Al-Gayyar et al., 2007; Battisti et al., 2008). Furthermore, oxidative stress can either inhibit or promote apoptosis, depending on the intensity of the oxidising stimuli. In fact, the apoptosis is induced by moderate oxidising stimuli and necrosis by an intense oxidising effect (Valko et al., 2006). There is evidence that constitutive activation of the MAPK and PI3K pathways occurs frequently in human cancer, possibly due to alteration of genes encoding key components of these pathways or upstream activation of cell-surface receptors resulting from mutations or amplification (Schubbert et al., 2007; Courtney et al., 2010). Deregulated signalling due to constitutive activation of these pathways might lead to uncontrolled cell growth and survival, resulting in oncogenic transformation and progression (De Luca et al., 2012).

Superoxide dismutase (SOD) and catalase are among the most efficient enzymatic antioxidants. Three types of SODs are present in human tissues: cytoplasmic Cu/Zn-SOD, extracellular Cu/ZnSOD (ecSOD), and mitochondrial MnSOD (Wan et al., 1994). MnSOD is synthesized in the cytoplasm and then driven into the mitochondrial matrix where it is subsequently cleaved into its mature and enzymatically active form. The data reported on antioxidant enzymes in different human cancer types are controversial. Furthermore, altered levels of antioxidant enzymes (SOD and CAT) and non-enzymatic antioxidants are evident in many human cancer cells (Mc Eligot et al., 2005). It has been shown that SOD and CAT activities are decreased in acute lymphoblastic leukemia (ALL) and chronic lymphocytic leukemia (Oltra et al., 2001). For example, CAT activity is reduced in LLA newly diagnosed patients, in remission induction and remission maintenance patients when compared to healthy subjects (Battisti et al., 2008). SOD expression levels among the various cancer types and stages display heterogeneity which may be related to both different optimal levels of oxidative stress among the

Conflict of interest: Dr. Aldo Mancini is the founder of Laedhexa Biotechnologies Inc.

*Correspondence to: Alessandra Pica, Department of Biology, University of Naples, Federico II, via Mezzocannone 8 (80134) Naples, Italy.
E-mail: alessandra.pica@unina.it

Manuscript Received: 9 April 2014
Manuscript Accepted: 22 September 2014

Accepted manuscript online in Wiley Online Library (wileyonlinelibrary.com): 7 October 2014.
DOI: 10.1002/jcp.24840

TABLE 1. Three-day-culture cell viability

	Cell concentration	Trypan blue	Morphology
T-leukemic cells			
T 0	1,000,000/mL	78%	NM. ND. Clump absent
T 1	400,000/mL	87%	NM. ND. Clump absent
T 2	400,000/mL	65%	NM. ID. Clump present
Jurkat cells	800,000/mL	100%	NM. ID. Clump present
Lymphocytes			
T 0	1,200,000/mL	100%	NM. ND. Clump absent
T 1	800,000/mL	90%	NM. ID. Clump absent
T 2	800,000/mL	70%	NM. ID. Clump present

NM, normal morphology; ND, normal density; ID, increased density.

various cancer types and the use of alternate pathways in response to oxidative stress.

A new isoform of MnSOD was recently discovered and isolated from the human liposarcoma cell line (LSA). LSA-type MnSOD differs from wild type human MnSOD by a single threonine to isoleucine substitution at amino acid 82, and its MW (around 30 kDa) is significantly higher than that of conventional MnSOD (24 kDa). Furthermore, unlike wild type MnSOD, which normally remains confined to the mitochondrial matrix (Hunter et al., 1997), LSA-type MnSOD is released from adipocytes into the medium (Mancini et al., 2006). As demonstrated by Mancini et al. (Mancini et al., 2008), recombinant LSA-type MnSOD (rMnSOD) has a distinctive capacity to penetrate and kill cancer cells expressing oestrogen receptors, without having cytotoxic effects on normal cells. The oncotoxic activity of rMnSOD is due to an increase in the level of oxidants both in tumor and leukemic cells, which contain low levels of catalase (Pica et al., 2010).

Recently mitochondrial alterations in cancer cells have been recognized as a target for cancer therapy (Barbosa et al., 2012). In spite of recent progress in therapy, approximately 25% of children and 50% to 70% of adults with T-ALL develop treatment resistant disease (Goldenberg et al., 2003), which carriers a poor prognosis (Bassan et al., 2004). In this study we assess rMnSOD biological function to determine its oncotoxic effect on pediatric high-risk T-ALL and Jurkat cells and its influence on apoptosis and cellular proliferation mediated by the MAPK and AKT pathway.

Materials and Methods

Reagents

The LSA-type MnSOD was isolated from human liposarcoma cell line (LSA) and obtained in recombinant form rMnSOD as reported by Mancini et al. (Mancini et al., 2006, 2008). rMnSOD was diluted in the medium of culture cells.

Culture cells

Lymphoblastic leukemia cells were collected from one patient diagnosed and treated for T-cell acute lymphoblastic leukemia (T-ALL) at the Pediatric Oncology Unit of Second University of Naples and purified by bone marrow using Ficoll Hystopaque density gradient centrifugation. Clinical characteristics of patient at diagnosis were: age 3 years old, white blood count 197000/μL, FAB classification L2, good prednisone responder and early T immunophenotype.

Leukemic lymphoblasts, Jurkat cells and lymphocytes from healthy donors (as control) were cultured at a density of 1×10^6 cells/mL in RPMI media supplemented with 1% Penstrep and 10% FBS in a humidified atmosphere containing 5% CO_2 at 37 °C.

Cell viability assay

Cell viability was analyzed by MTT [3-(4, 5-dimethylthiazol-2-yl)-2, 5-diphenyl tetrazolium bromide] assay. Cells were seeded in 96-well plates at the density of 1×10^3cells/well in a final volume of 100 μL. Cells were then incubated at 37 °C in a humidified atmosphere to allow exponential growth. After 72 h of growth, cells were treated with rMnSOD at a final concentration ranging from 0.0067 μM to 0.67 μM, for 5 h. At 5 h from the treatment, cells were exposed to 10% MTT for 3 h at 37 °C to form

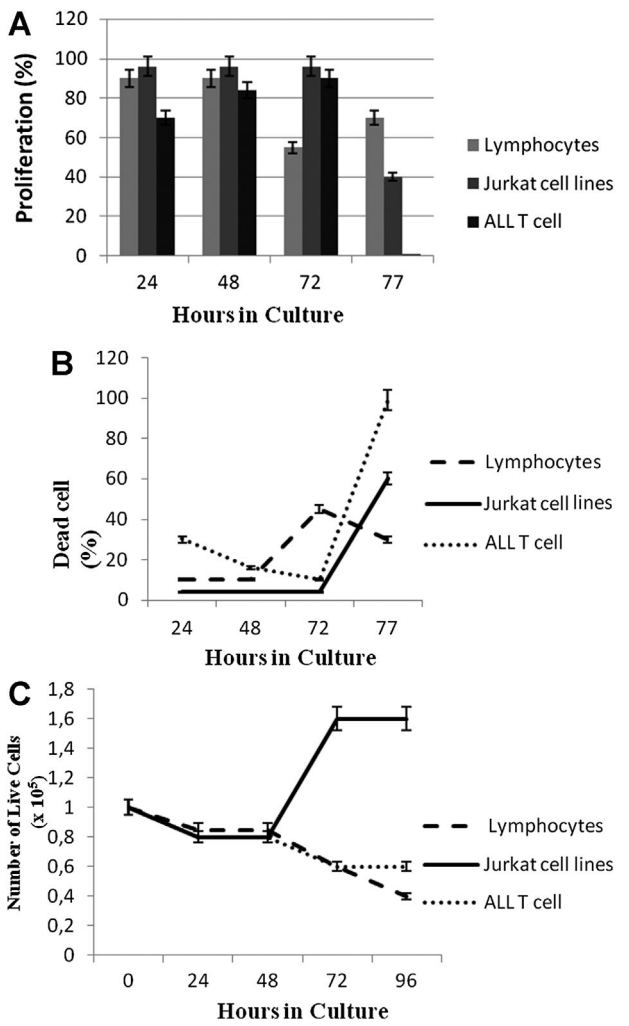

Fig. 1. Proliferation assay and growth inhibition. (A) Survival of T-ALL cells, Jurkat cells and lymphocytes, by using MTT analysis, after 72 h of growth, and following treatment with 0.067 μM rMnSOD for 5 h. (B) Cell viability by Trypan Blue exclusion assay. Results are the average of three independent experiments. (C) Spontaneous proliferation curve of Jurkat cells line, T-ALL and lymphocytes after 96 h of growth.

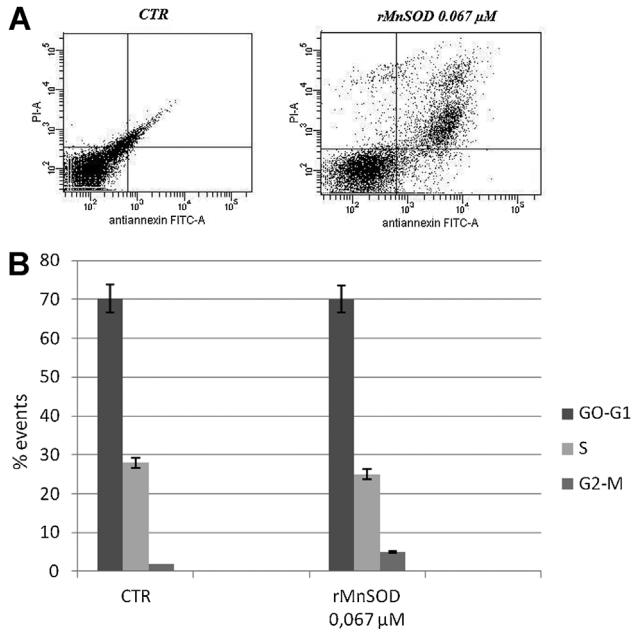

Fig. 2. Effect of rMnSOD on apoptosis induction. (A) FACS analysis after double labeling of Jurkat cells with PI and Annexin V following treatment with 0.067 μM rMnSOD, compared to the control. (B) Distribution of Jurkat cells in the different phases of the cell cycle after treatment with 0.067 μM rMnSOD.

formazan crystals by reacting with metabolically active cells. The formazan crystals were solubilized in a 1 N isopropanol/HCL 10% solution at 37 °C for 30 min. The absorbance at 595 nm was then determined. Cell viability was determined by the formula: Cell viability of the treated wells—absorbance of the blank control wells)/(absorbance of the negative control wells—absorbance of the blank control wells) x 100%. Control cells (leukemic lymphoblasts, Jurkat cells and lymphocytes) were cultured under identical conditions but in the absence of rMnSOD. All experiments were performed in triplicate.

Cell cycle analysis

Jurkat cells were seeded at density of 1×10^6 and then incubated 24 h in humidified atmosphere at 37 °C. The next day, the cells were treated with 0.067 μM rMnSOD for 5 h in humidified atmosphere at 37 °C. After incubation, cells were washed in PBS 1×, pelleted, and stained with Propidium Iodide (PI) solution (50 mg PI in 0.1% Sodium citrate, 0.1% NP40, pH 7.4) for 30 min at 4 °C in the dark. Flow cytometry analysis was performed using a FACScan flow cytometer (Becton Dickinson, San Jose, CA). To evaluate cell cycle, PI fluorescence was collected as FL2 (linear scale) by the ModFIT software (Becton Dickinson). The intracellular DNA content evaluation, was performed by analyzing 20000 events for each point in triplicate. Each experiment gave a S.D. less than 5%.

Evaluation of apoptosis by DNA-flow cytometry

Apoptotic cell death was analyzed by Annexin-V-FITC staining. Annexin-V-FITC binds to phosphatidylserine residues, which are translocated from the inner to the outer leaflet of the plasma membrane during the early stages of apoptosis. Apoptotic cell labeling was performed using an Annexin-V kit (MedSystems Diagnostics, Wien, Austria). Jurkat cells were seeded at the density 1×10^6 and then incubated 24 h in humidified atmosphere at 37 °C. Then the cells were treated with 0.067 μM rMnSOD and incubated at 37 °C for 5 h. After the incubation the cells were collected and centrifuged for 5 min at 1,500 rpm. Pellet was washed in PBS 1×, incubated with Annexin-V-FITC in a binding buffer (10 mM HEPES, pH 7.4, 150 mM NaCl, 5 mM KCl, 1 mM MgCl2, 2.5 mM CaCl2) for 30 min at 4 °C. Analysis of apoptotic cells was performed by flow cytometry (FACScan, Becton Dickinson). 10×10^4 events were acquired for each sample. Analysis was carried out in triplicate.

Immunocytochemistry at light microscopy

Lymphoblastic leukemia cells, Jurkat cells, and lymphocytes were incubated for 5 h in the presence or absence of rMnSOD at a final concentrations ranging from 0.0067 to 0.67 μM. Subsequently, a cytospin was used to smear cells onto slides. The smears were fixed in Zamboni solution (4% paraformaldehyde, 15% picric acid) for 60 min and then washed with 1× PBS and incubated for 5 min with 3% hydrogen peroxide to quench endogenous peroxidase activity. Immunostaining was performed using the DAKO LSA+ System HRP kit. Rabbit anti-rMnSOD-Lp (1:200), was incubated on slides for 30 min, followed by incubation with the biotinylated secondary antibody for 30 min and peroxidase-labeled streptavidin for 30 min. To complete the reaction, a substrate-chromogen solution was used. The smears were counterstained with hematoxylin.

Determination of the apoptotic index

Apoptotic cells and bodies were counted from several areas of each sample. The apoptotic index (AI) was estimated as the number of apoptotic cells and/or bodies per 1,000 tumor cells, expressed in percentages.

Immunogold method at transmission electron microscopy

Both leukemic cells and lymphocytes were incubated for 6 h in the presence or absence of rMnSOD at a final concentration ranging from 0.0067 to 0.67 μM. The cells were then fixed using 0.1% glutaraldehyde and 4% paraformaldehyde in 0.1 M sodium cacodylate buffer for 60 min at room temperature and washed twice in 0.1 M sodium cacodylate buffer. Samples were then treated with 1% OsO4 for 10 min, dehydrated, embedded in Epon 812, and polymerized at 60 °C for 24 h. Ultrathin sections were prepared using a Leica Ultracut UCT ultramicrotome and mounted on nickel grids. The sections were subsequently subjected to antigen unmasking in citrate buffer, incubated with 10% hydrogen peroxide for 10 min, washed 3 times in PBS 0.9% for 5 min, and incubated in BSA 1% and glycine 0.15% in PBS for 30 min. The samples were incubated with polyclonal rabbit anti-rMnSOD-Lp (1:20) in Tris-HCl 0.05 mol/L with 1% BSA overnight at 4 °C,

TABLE 2. Cell cycle analysis

	UL necrosis	UR late apoptosis	LL living cells	LR early apoptosis
CTR	3.8	5	90.8	0.4
rMnSOD 0.067 μM	2.5	23.7	67.1	6.6

UL, upper left (necrosis); UR, upper right (late apoptosis); LL, lower left (viable); LR, lower right (early apoptosis); CTR, Untreated cells.
Insets, % of positive cells.

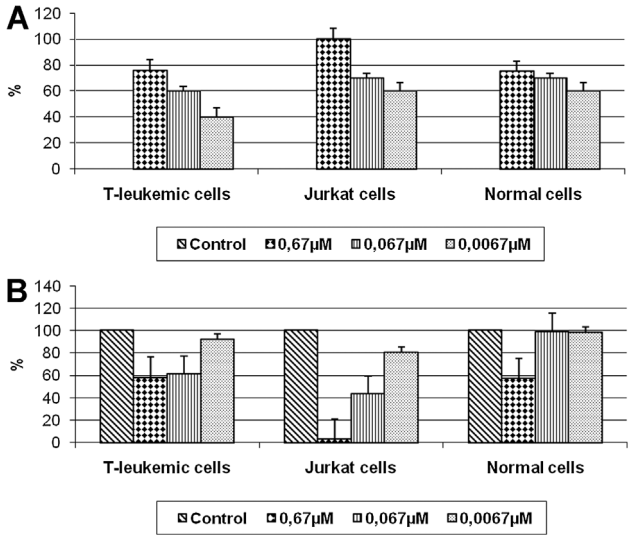

Fig. 3. (A) Percentage of labeled cells at light microscopy. (B) Trypan Blue test after the treatments with the different concentrations of rMnSOD for 5 h. The controls displayed no labeling.

washed three times in PBS 0.9% for 10 min, and incubated with a donkey anti-rabbit secondary antibody conjugated to 15 nm colloidal gold diluted (1:10) in 0.1% BSA for 2 h at room temperature. The sections were washed in PBS (pH 7.4) and distilled water prior to counterstaining with uranyl acetate and lead citrate. Ultrathin sections were examined using a LEO 912AB Zeiss transmission electron microscope.

Protein extraction and western blot analysis

Protein extraction was performed on ice for 30 min using lysis-buffer (1M Tris-HCl pH 8, 5 M NaCl, 0.5 M NaF, 100% NP40) with protease-inhibitors (4 μL/mL PMSF, 2μL/mL aprotinin and pepstatin, 1 μL/mL Na Ortovanadate). Cell lysates were centrifuged at 20,000 g for 2 min at 4 °C, and proteins were extracted from supernatant. Total protein concentration was determined using Bradford assay (Bio-Rad). For Western blot analysis, 30 μg of total protein was run on 10% polyacrylammide gel and blotted onto PVDF membrane (Millipore, Marlborough, MA). The membrane was blocked in 5% nonfat dry milk dissolved in TBS buffer (2 mM Tris, 13.7 mM NaCl, 0.1% tween-20, pH 7.6) overnight. All washes were performed in TBS buffer. Immunoblotting was performed using primary antibodies against Bcl-2 (100), Bax (N20), AKT (H-136), pAKT (Ser473), ERK (G-12), and pERK (E-4) (Santacruz Biotechnology, INC) (1:500) incubated for 1 hour. Secondary antibodies (Santacruz Biotechnology 1:5000) were incubated at room temperature for 1 hour. Bands were visualized using a chemiluminescent system (ECL-Amersham). The intensity of each band was acquired with a CCD camera and analyzed with Quantity One 1-D analysis software (Biorad Laboratories). Results were normalized against the level of α-actin expression in each sample.

Detection of reactive oxygen species

Cell samples were pretreated with or without 10 mM NAC (Sigma—Aldrich, Saint Louis) at 37 °C for 20 min, and incubated with 0.067 μM rMnSOD for 5 h, then the cells were washed with PBS 1×

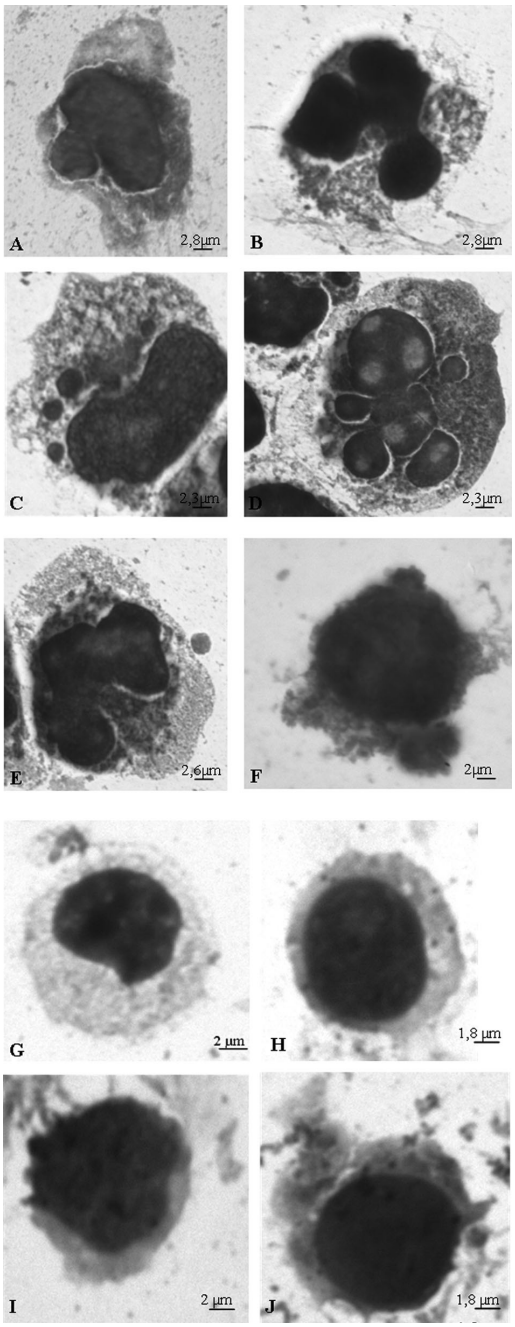

Fig. 4. Jurkat cells treated with increasing concentrations of rMnSOD. All cells of the panel display an intense brown cytoplasmic and nuclear immunoreaction to anti-rMnSOD, revealed by diaminobenzidine reaction: A) 0,0067 μM rMnSOD produces only mild pre-apoptotic changes such initial nuclear and cytoplasmic fragmentations, while 0.067 μM rMnSOD (B, C, D, and E) lead to a clear and advanced both nuclear and cytoplasmic apoptotic fragmentation and finally 0.67 μM rMnSOD (F) is a concentration that, very likely, exceeds the capacity of the cell redox, leading to plasma membrane ruptures. (G-J) Lymphocytes treated with increasing concentrations of rMnSOD. All cells display an intense brown cytoplasmic and nuclear immunoreaction to anti-rMnSOD, revealed by diaminobenzidine reaction: G) control cell; H) and I) cells respectively treated with 0.0067 and 0.067 μM rMnSOD, showing a condition of well-being without any signs of apoptosis; J) cell treated with 0.67 μM rMnSOD displaying plasma membrane rupture. Very likely, this is a concentration that exceeds the capacity of the cell redox.

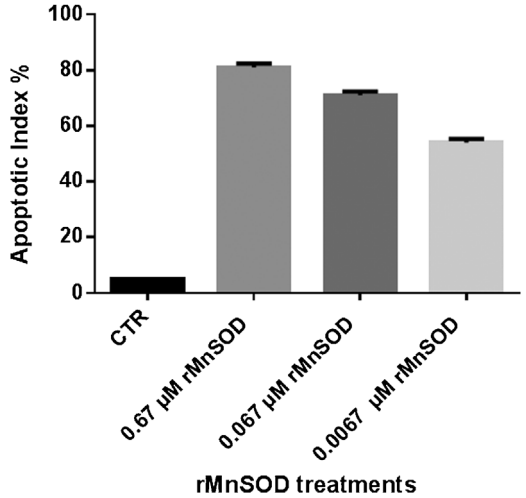

Fig. 5. Apoptotic index percentages of apoptotic Jurkat cells following rMnSOD treatments.

and incubated with 10 μM 2′,7′-dichlorodihydrofluorescein diacetate (DCFH-DA-Cayman, Baverno, Italy) at 37 °C for 20 min. DCFH-DA diffused into cells is deacetylated by cellular esterases to non-fluorescent 2′, 7′-Dichlorodihydrofluorescin (DCFH), which is rapidly oxidized to highly fluorescent 2′, 7′-Dichlorodihydrofluorescein (DCF) by ROS. The fluorescence intensity is proportional to ROS levels within the cell cytosol; the fluorescence intensity was assessed using a Hitachi (Model U-2000) double-beam spectrofluorimeter with excitation at 484 nm and emission at 530 nm. Background fluorescence (conversion of DCFH-DA in absence of homogenate) was corrected by the inclusion of parallel blanks.

Results

Effects of rMnSOD on growth inhibition on human T-ALL cells, Jurkat cells and lymphocytes

Cells were cultured and monitored for 3 days to assess cellular concentration and proliferation using Trypan blue exclusion assay and MTT tests (Table 1).

To perform the experiments with the optimal dose of rMnSOD, we initially determined the dose-dependent survival rate of Jurkat and T-ALL upon rMnSOD treatment. We observed, based on Trypan blue exclusion assay and MTT tests, a less than 5% cell death after 5 h treatment with 0.003 μM rMnSOD, whereas a significant reduction in cell viability (by∼30%, data not shown) was induced by a 5 h treatment with 0.067 μM rMnSOD. Thus, 0.067 μM rMnSOD was selected for the subsequent experiments to minimize the apoptosis-induced alteration in protein expression.

In details, after 72 h of growth, cells were treated with 0.067 μM rMnSOD for 5 h in culture. We observed, with MTT test, a proliferation rate of 1% T-ALL cells, 40% Jurkat and 70% lymphocytes (Fig. 1A). Moreover with Trypan blue exclusion assay, performed in the same conditions, we observed a growth inhibition of 99% T-ALL cells, 60% Jurkat and 30% lymphocytes (Fig. 1B). Spontaneous proliferation curves of Jurkat cells line, T-ALL and lymphocytes were used as normalized controls. These curves showed an increase of Jurkat cell's growth, a decrease of lymphocyte growth after 48 h and a slight decrease followed by a stabilization of T-cell ALL's growth after 48 h to 96 h (Fig. 1C).

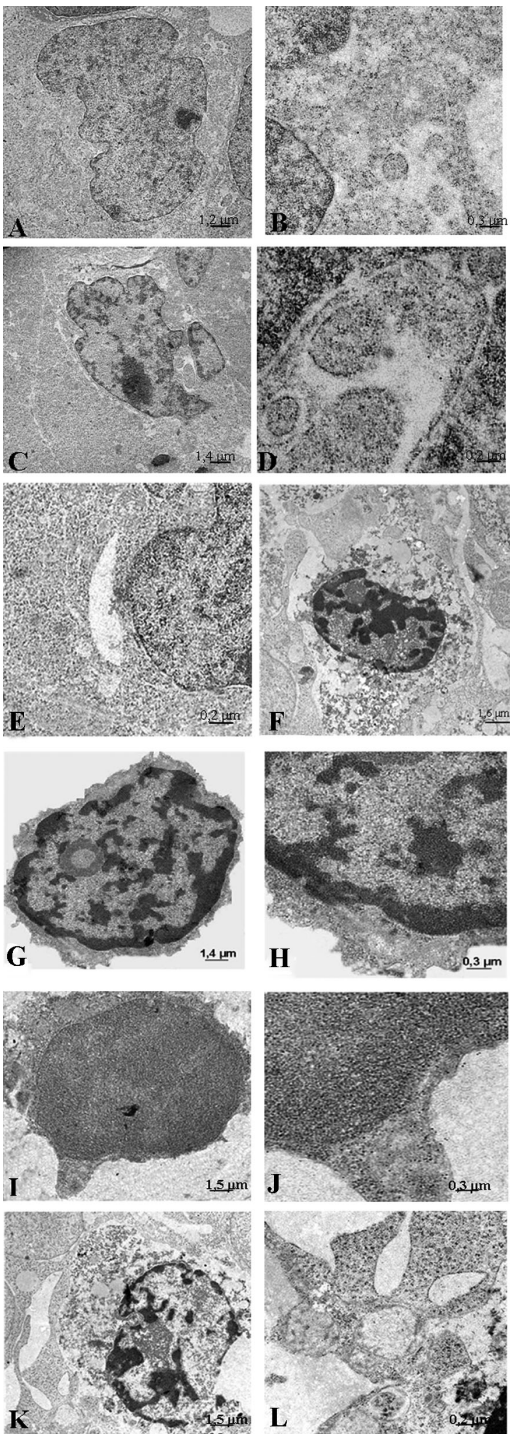

Fig. 6. Jurkat cells by TEM following immunoreaction with anti-rMnSOD revealed by 15 nm colloidal gold particles: A-B) cell treated with 0.0067 μM rMnSOD showing an initial pre-apoptotic nuclear incision and slight cytoplasmic fragmentation; C) and D) cell treated with 0.067 μM rMnSOD which lead to a clear nuclear and cytoplasmic apoptotic fragmentations; E-F) cell treated with 0.67 μM rMnSOD, that shows membrane rupture. Lymphocytes treated with increasing concentrations of rMnSOD respectively followed by immunorevealing with anti-rMnSOD and 15 nm colloidal gold particles. G) and H) Control cells; I) and J) lymphocytes treated with 0.067 μM rMnSOD displaying a well-being condition while in K) and L) lymphocytes treated with 0.67 μM rMnSOD show cell damage.

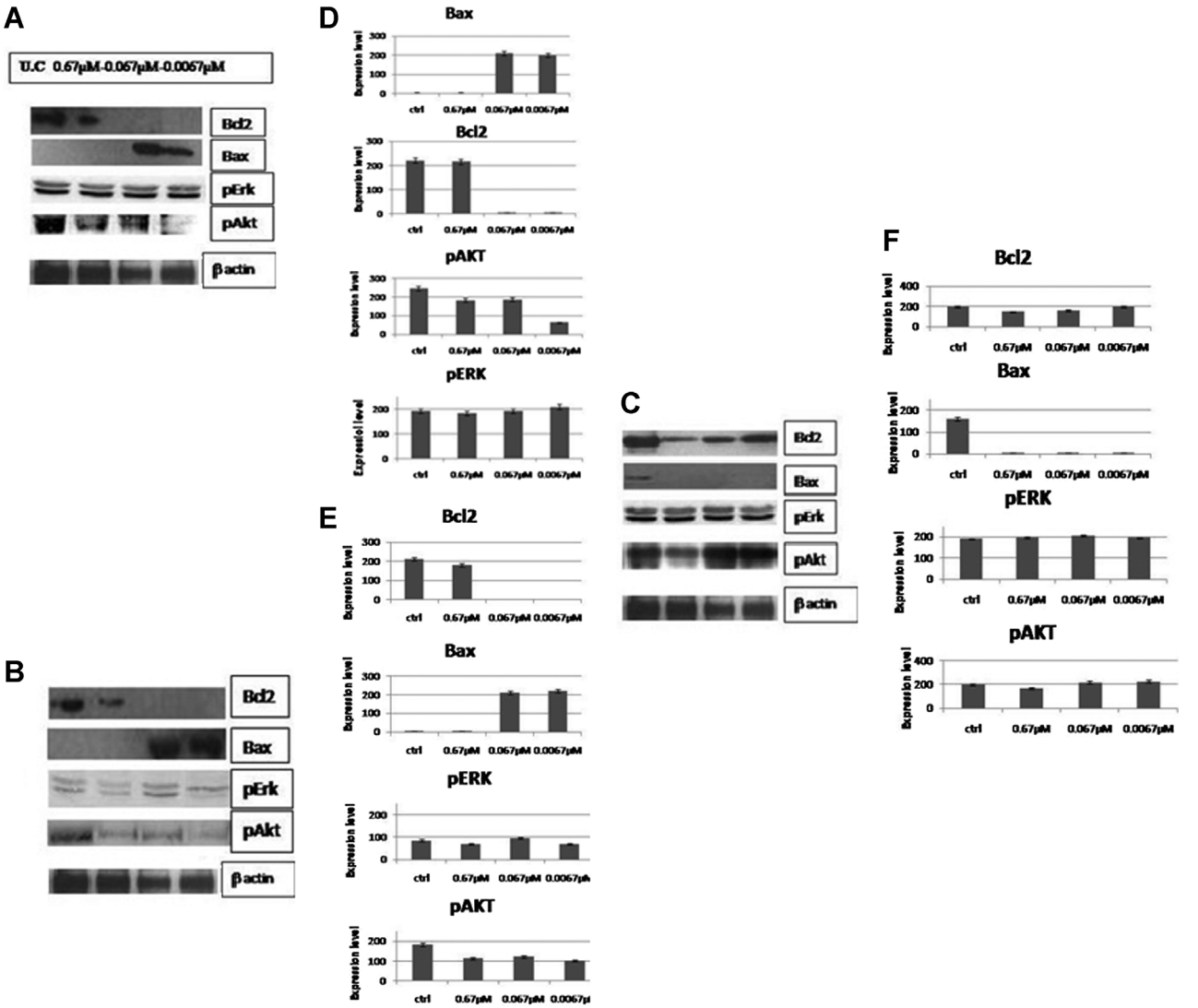

Fig. 7. Western Blot Assay and software analysis of proteins expression: T-ALL cells (A), Jurkat cell line (B) and lymphocytes (C) were processed for the determination of Bcl-2, Bax, the phosphorylation of ERK and AKT after rMnSOD treatment at a final concentration ranging from 0.0067 to 0.67 μM. The experiments were performed at least three different times and the results were always similar. UC: untreated cells. Scan of the bands associated with expression of Bcl-2, Bax, pERK and pAKT in T-ALL (D), Jurkat (E) and lymphocytes (F) normalized with the house-keeping protein, was performed with a dedicated software and the intensities of the bands were expressed as arbitrary units (%, mean of three different experiments).

Effect of rMnSOD on apoptosis induction

After the treatment with 0.067 μM rMnSOD, we evaluated the induction of apoptosis on Jurkat cells by FACS analysis, after staining with Annexin-V-FITC and PI, as above described. As shown in Figure 2 and Table 2, a significant increase of apoptotic cells compared to control cells has been detected. In details, we found that the treatments with 0.067 μM rMnSOD for 5 h induced apoptosis in 23.7% of Jurkat cells, compared to 5% untreated cells.

Light microscopy

The treatments performed respectively with 0.0067, 0.067 and 0.67 μM rMnSOD for 5 h on the three cell populations gave the following percentages of labeled cells: 40%, 60% and 76% of cultured leukemic T cells; 60%, 73% and 100% of Jurkat cells and 60%, 70% and 75% of lymphocytes, while the controls displayed no labeling (Fig. 3A). Overall, these results indicate that most cells internalized rMnSOD, as they displayed both mainly cytoplasmic and less nuclear immunoreactivity (Fig. 4 A–F, H–J). The percentages of viability as a result of the three concentrations of rMnSOD tested are reported in Figure 3B.

Leukemic T-cell and Jurkat cells

The T leukemic cells and Jurkat cells, treated with 0.67 μM rMnSOD, displayed cytoplasmic and nuclear positivity as well as rupture of the plasma membrane, (Figs. 4 F, 6E–F). In contrast, both the cells treated with 0.0067 and 0.067 μM rMnSOD showed cytoplasmic positivity as well as the pre-apoptotic changes of early and complete nuclear and cytoplasmic fragmentation (Figs.4 A–E, 6A–D).

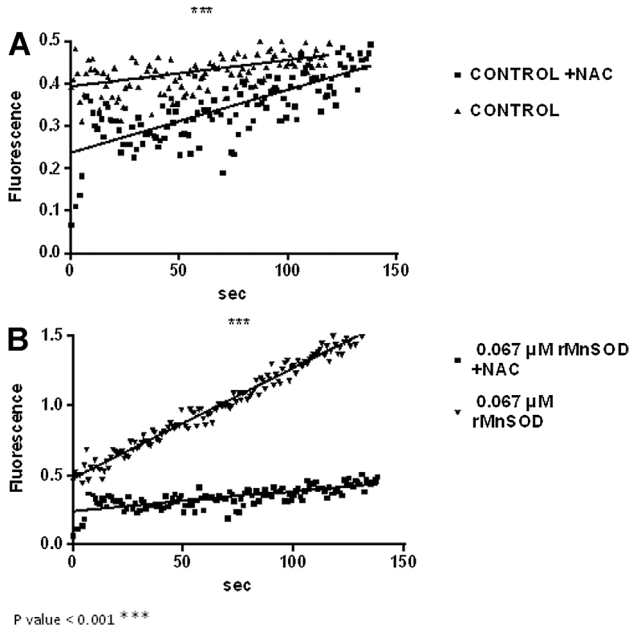

Fig. 8. Spectrofluorimetric analysis of reactive oxygen species. (A) Control Jurkat cells treated with or without NAC. (B) Jurkat cells pre-incubated with or without NAC and then with rMnSOD. Results are the means of three experiments.

Lymphocytes

Lymphocytes treated with 0.67 μM rMnSOD showed cytoplasmic and slight nuclear positivity as well as rupture of the plasma membrane (Figs. 4J, 6K–L); whereas cells treated with 0.0067 or 0.067 μM rMnSOD showed no morphological alterations (Figs. 4H–J, 6I–L). Lymphocytes (not treated with rMnSOD) displayed no positivity (Figs. 4G, 6G–H). Together, these findings indicate that 0.0067 and 0.067 μM rMnSOD cause apoptosis of only leukemic cells, instead 0.67 μM rMnSOD is a toxic concentration.

Determination of the apoptotic index

The number of the cells displaying both apoptotic nuclear and cytoplasmic fragmentation is reported in Figure 5.

Transmission electron microscopy

We used transmission electron microscopy (TEM) to confirm the internalization of rMnSOD by leukemic T cells, Jurkat cells, and lymphocytes treated with 0.0067, 0.067 and 0.67 μM of rMnSOD. Our TEM results show colloidal gold particles (10 nm) dispersed mainly in the cytoplasm and sometimes near the mitochondrial envelope (Figs. 6 A–F, I–L), confirming that rMnSOD enters the cells. The internalization of rMnSOD was also evident in nuclear and cytoplasmic apoptotic fragments (Figs. 6 C–D) and in damaged cells (Figs. 6 E–F). rMnSOD also enters lymphocytes, as indicated by the presence of the 10 nm-gold particles distributed in the cytoplasm (Figs. 6 I–L) after the 5 h treatment. No labeling was observed in untreated cells (Figs. 6 G–H).

rMnSOD treatment on survival pathway

To determine the mechanism of growth inhibition by rMnSOD in more details, we analyzed the apoptotic profile after treatment with rMnSOD. In particular we evaluate expression of Bcl-2 and Bax in leukemic T cells, Jurkat cells, and lymphocytes at a final concentration ranging from 0.0067 to 0.67 μM of rMnSOD.

The treatment of leukemic T cells with 0.067 μM rMnSOD induces the expression of pro-apoptotic Bax and suppresses expression of Bcl-2 in comparison to non-treated cells (Fig. 7 A–D). Jurkat cells treated with 0.067 μM rMnSOD also showed increased expression of Bax and decreased expression of Bcl-2 (Fig. 7 B–E). Conversely, the treatment of lymphocytes with 0.067 μM rMnSOD did not affect Bcl-2 or Bax expression in comparison to non-treated counterparts (Fig. 7 C–F).

rMnSOD treatment on proliferation pathway

To analyze if rMnSOD acts also on key regulators of proliferation pathways, we asses AKT and ERK phosphorylation respect to basal levels. We founded that rMnSOD treatment did not affect AKT phosphorylation in all tested samples. No changes in the expression of phosphorylated ERK, following rMnSOD treatment, resulted in T-ALL cells and in lymphocytes (Fig. 7 A, C), while a slightly decreased expression of phosphorylated ERK was detected in Jurkat cells (Fig. 7B), thus indicating that growth inhibition after rMnSOD treatment could be not influenced by MAP/ERK chinase pathway but by apoptotic pathway, except for Jurkat cells that are a model with altered multiple pathways.

Detection of reactive oxygen species

N-acetylcysteine (NAC) resulted in blocking of rMnSOD-induced ROS generation, as shown in Figure 8. In fact 10 mM NAC induced a DCF decrease, following incubation with 0,067 μM rMnSOD, while the treatment without NAC, showed fluorescence comparable to the control. These data suggest that 0.067 μM rMnSOD induces ROS production in much higher amounts than in controls, as expected.

Discussion and Conclusions

It is well known that leukemic cells produce high levels of reactive oxygen species and have a disturbance of the protective role of enzyme against free radical. This variability of cell antioxidant machinery and ROS production, according to the cancer type, may be explained by the level of antioxidant defense which lead to a ROS production effective in generating neoplastic cell transformation but not enough to trigger apoptosis. Increasing evidence demonstrates the key role of ROS in the regulation of cell life and death. The toxic potential of ROS is able to activate the immune response.

Thus, the development of new therapeutic interventions must deal with the duality of ROS in both protective cytotoxic against "non self" action and injurious action of their exceeding accumulation able to induce carcinogenesis (Manda et al., 2009). Similarly the rMnSOD shows a duality of action too, being able to trigger apoptotic death of cancer cells while oxygenates the healthy cells, or, if it exceeds the ability of catalase to transform the peroxide into oxygen and water, can induce necrosis in both tumor cells and healthy cells (Mancini et al., 2006). So the redox balance appears to be the main mechanism of carcinogenesis control (Manda et al., 2009 Barbosa et al., 2012). The rMnSOD used in the present study, was previously demonstrated to exert oncosuppressive activity in vitro and in vivo on tumor cells expressing oestrogen receptors (Mancini et al., 2006). The effect of internalized rMnSOD was hypothesized to be the increase of oxidant levels which are known to mediate cell killing (Mashiba and Matsunaga, 1998; Mainous et al., 2005).

In this study, we demonstrated that rMnSOD treatment induce apoptosis in both cultured ALL patient cells and in Jurkat

cell line, without adverse effects on lymphocytes. In fact we showed that 0.067 μM rMnSOD causes apoptosis of leukemic T cells and of Jurkat cells in vitro and we observed (by MTT assay) a survival rate of 1% T-ALL cells, 40% Jurkat and 70% lymphocytes after treatment with rMnSOD. Moreover, we showed that 0.067 μM rMnSOD up regulates the pro-apoptotic protein Bax and inhibits the anti-apoptotic protein Bcl-2 in leukemic T cells. This data are in accordance with Mancini et al. (Mancini et al., 2006) on breast cancer cells who confirm a strong up regulation of pro-apoptotic Bax gene expression in the presence of rMnSOD, suggesting that this treatment might induce the apoptotic cascade. The possible involvement of an apoptotic mechanism was suggested by the strong inhibition of anti-apoptotic Bcl-2 gene expression detected in tumor cells in the presence of rMnSOD (Mancini et al., 2008). In addition, FACS analysis of cells treated with 0.067 μM rMnSOD displayed an evident increase of apoptotic cells in 23.7% of Jurkat cells, as compared to control cells.

Interestingly, leukemic cells internalize the exogenous rMnSOD that converts free radicals present in H_2O_2. Notably, catalase detoxifies H_2O_2 into molecular oxygen and it is usually in lower amount in leukemic cells than in healthy cells. (Battisti et al., 2008). Thus, treatment with rMnSOD may lead to accumulation of H_2O_2 and subsequent death of leukemic cells. In contrast, lymphocytes do not show this reduction in catalase activity and can tolerate high levels of endogenous H_2O_2 production. However, a concentration of 0.67 μM rMnSOD is toxic to leukemic cells and to lymphocytes; in fact at this concentration the rMnSOD induces necrosis due to a stechiometric imbalance that is created between the enzymes MnSOD and catalase. In conclusion, our findings suggest that rMnSOD could be considered as an associated additional treatment for leukemia, particularly as low concentrations of rMnSOD seem specifically toxic to cancer cells while having a protective effect on healthy cells. According to the current knowledge about the therapeutic target role of the redox balance (Manda et al., 2009; Barbosa et al., 2012), these results suggest an action for the rMnSOD which would achieve a good therapeutic efficiency and no side effects.

Acknowledgments

This work was partially supported by AIL (Italian Association against Leukemia-Lymphoma and Myeloma Division "Valentina Picazio" and partially by AGOP (Parent Association Pediatric Oncology). TEM observations have been performed at Zoological Station of Naples Anton Dohrn: the authors are grateful to Franco Iamunno for his technical assistance. The authors are grateful to the "Lega Italiana Per La Lotta Contro I Tumori di Napoli" for their partial financial support.

Literature Cited

Al-Gayyar MM, Eissa LA, Rabie AM, El. Gar AM. 2007. Measurements of oxidative stress status and antioxidant activity in chronic leukemia patients. J Pharm Pharmacol 59: 409–417.

Barbosa IA, Machado NG, Skildum AJ, Scott PM, Oliveira PJ. 2012. Mitochondrial remodeling in cancer metabolism and survival: Potential for new therapies. Bioch Biophys Acta 1826:238–254.

Battisti V, Maders LD, Bagatini MD, Santos KF, Spanevello RM, Maldonado PA, Brulé AO, Araújo Mdo, Schetinger C, Morsch MR. 2008. Measurement of oxidative stress and antioxidant status in acute lymphoblastic leukemia patients. Clin Biochem 41: 7–8.

Bassan R, Gatta G, Tondini C, Willemze R. 2004. Adult acute lymphoblastic leukemia. Crit Rev Oncol Hematol 50:223–261.

Cooke MS, Evans MD, Dizdaroglu M, Lunec J. 2003. Oxidative DNA damage: Mechanisms, mutation, and disease. FASEB J 171195–1214.

Courtney KD, Corcoran RB, Engelman JA. 2010. The PI3K pathway as drug target in human cancer. J Clin Oncol 28:1075–1083.

De Luca A, Maiello RM, D'Alessio A, Pergameno M, Normanno N. 2012. The RAS/RAF/MEK/ERK and the PI3K/AKT signaling pathways: Role in cancer pathogenesis and implications for therapeutic approaches. Expert Opin Ther Targets 16: 17–27.

Goldenberg JM, Silverman LB, Levy DE, Dalton VK, Gelber RD, Lehmann L, Cohen HJ, Sallan SE, Asselin BL. 2003. Childhood T-cell acute lymphoblastic leukemia: The Dana-Farber Cancer Institute acute lymphoblastic leukemia consortium experience. J Clin Oncol 21:3616–3622.

Hunter T, Bannister WH, Hunter GJ. 1997. Cloning, expression and characterization of two Manganese Superoxide Dismutase from Caenorhabditis elegans. J Biol Chem 272: 28652–28659.

Mainous AG, III, Wells BJ, Koopman RJ, Everett CJ, Gill JM. 2005. Iron lipids, and risk of cancer in the Framingham Offspring cohort. Am J Epidemiol 161:1115–1122.

Malyszczak K, Tomasz W, Mazur G, Lindner K, Pyszel A, Kiejna A, Kuliczkowski K, Andrzejak R. 2005. Anxiety and depressive symptoms in patients treated due to haematologic malignancies. Psychiatr Pol 39:33–40.

Mancini A, Borrelli A, Schiattarella A, Fasano S, Occhiello A, Pica A, Sehr P, Tommasino M, Nuesch JP, Rommelaere J. 2006. Tumor suppressive activity of variant isoform of manganese superoxide dismutase released by a human liposarcoma cell line. Int J Cancer 119:932–943.

Mancini A, Borrelli A, Schiattarella A, Aloj L, Aurilio M, Morelli F, Pica A, Occhiello A, Lorizio R, Mancini R, Sica A, Mazzarella L, Sica F, Grieco P, Novellino E, Pagnozzi D, Pucci P, Rommelaere J. 2008. Biophysical and biochemical characterization of a liposarcoma-derived recombinant MnSOD protein acting as an anticancer agent. Int J Cancer 123:2684–2695.

Manda G, Nechifor MT, Neagu TM. 2009. Reactive oxygen species, cancer and anti-cancer therapies. Curr Chem Biol 3:342–366.

Mashiba H, Matsunaga K. 1988. Device for intracellular increase of oxygen free radicals and inhibition of MethA tumor cell proliferation: In vitro and in vivo studies. Int J Tissue React 10:273–280.

McEligot AJ, Yang S, Meyskens F. 2005. Redox regulation by intrinsic species and extrinsic nutrients in normal and cancer cells. Annu Rev Nutr 25:261–295.

Oltra AM, Carbonell F, Tormos C, Iradi A, Saez GT. 2001. Antioxidant enzyme activities and production of MDA and 8-oxo-dg in chronic lymphocytic leukemia. Free Radic Biol Med 30:1286–1292.

Pica A, Di Santi A, Basile F, Iacobellis F, Borrelli A, Schiattarella A, Mancini R, Mancini A. 2010. Anti-Cancer, anti-necrotic and imaging tumor marker role of a novel form of manganese superoxide dismutase and its leader peptide. Int J Biol Biomed Eng 4:53–60.

Skarstein J, Aass N, Fossa SD, Skovlund E, Dahl AA. 2000. Anxiety and depression in cancer patients: relation between the Hospital anxiety and depression scale and the European organization for Research and treatment of cancer core quality of life questionnaire. J Psychosom Res 49:27–34.

Schubbert S, Shannon K, Bollag G. 2007. Hyperactive Ras in developmental disorders and cancer. Nat Rev Cancer 7:295–308.

Valko M, Rhodes CJ, Moncol J, Izakovic M, Mazur M. 2006. Free radicals, metals and antioxidants in oxidative stress-induced cancer. Chem Biol Interact 160: 1–40.

Wan XS, Devalaraja MN, St Clair DK. 1994. Molecular structure and organization of the human manganese superoxide dismutase gene. DNA. Cell Biol 13: 1127–1136.